SAND99-3058C

FANTM, THE FIRST ARTICLE NIF TEST MODULE *

David L. Smith, J. Michael Wilson+, Henry C. Harjes, and William B. S. Moore+
Sandia National Laboratories#
P. O. Box 5800, Albuquerque, NM 87185-1184

Jud Hammon
Maxwell Physics International
2700 Merced St., San Leandro, CA 94577

Abstract

Designing and developing the 1.7 to 2.1-MJ Power Conditioning System (PCS), that will power the flashlamps of the main and power amplifiers for the National Ignition Facility (NIF) lasers, is one of several responsibilities assumed by Sandia National Labs (SNL) in support of the NIF Project. Maxwell Physics International has been a partner in this process. The NIF is currently being constructed at Lawrence Livermore National Labs (LLNL). The test facility that has evolved over the last three years to satisfy the project requirements is called FANTM, for the First Article NIF Test Module. It was built at SNL and operated for about 17,000 shots to demonstrate component performance expectations over the lifetime of NIF. A few modules similar to the one shown in Fig. 1 will be used initially in the amplifier test phase of the project. The final full NIF system will require at least 192 of them in four capacitor bays.

This paper briefly summarizes the final design of the FANTM facility and compares its performance with the predictions of circuit simulations for both normal operation and fault-mode response. Applying both the measured and modeled power pulse waveforms as input to a physics-based, semi-empirical amplifier gain code indicates that the 20-capacitor PCS can satisfy the NIF requirement for an average gain coefficient of 5.00 %/cm and can exceed 5.20 %/cm with 24 capacitors.

I. FANTM PULSED POWER DESIGN

The FANTM bank consists of 20 (24 max) 86-kJ, nominally 300-μF capacitors that are operated in parallel near 24 kV. Each capacitor (C in Fig. 1) is isolated from the rest of the bank by a current-limiting damping element (D), which is a 25-mΩ, 9-μH resistive coil. They connect to a single bus (B) that feeds the gas switch (S). The single ST300A air-insulated switch transfers over 500-kA peak current in a 300-μs FWHM critically damped pulse from the bank into 20 parallel output lines. Each of these lines is composed of a matched ballast inductor (I), an RG 220/U coaxial cable (L), which is 47.6-m long, and either a dummy resistive load or a pair of series-connected flashlamps. The full NIF will also include modules with a range of output cable lengths from 20 to 55 m, due to the different locations of the PCS modules with respect to the laser amplifiers. The main bank module has a weight of approximately 7 metric tons, a footprint of about 1.52 by 3.35 m, and a total height of about 3.11 m. A flashlamp pre-ionization pulse from a smaller 50-kJ Pre-Ionization/Lamp Check (PILC) parallel bank precedes the main pulse by a few hundred microseconds. A simplified circuit schematic of the system is shown in Figure 2.

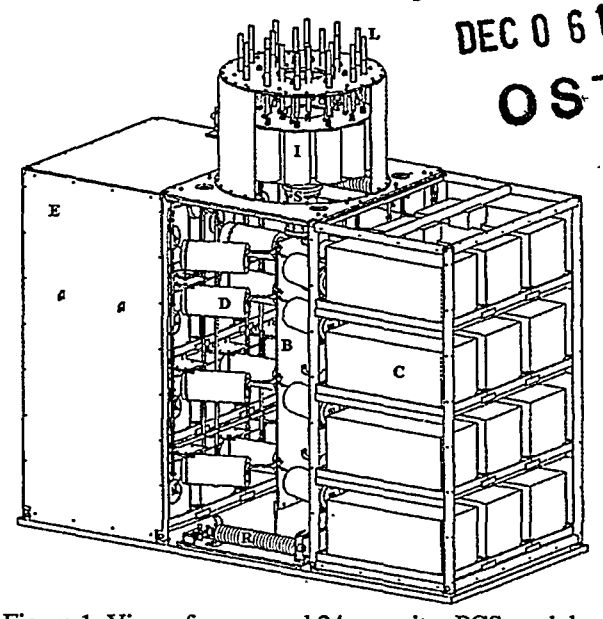

Figure 1. View of uncovered 24 capacitor PCS module.

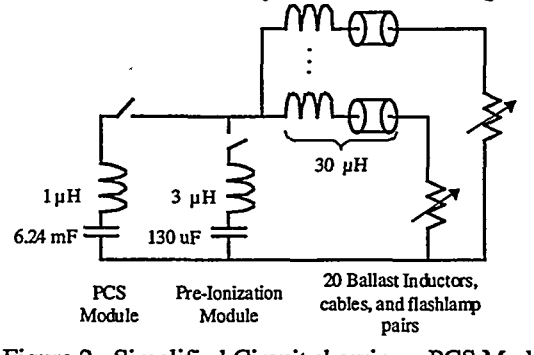

Figure 2. Simplified Circuit showing a PCS Module and PILC driving flashlamp loads, for the 20-capacitor PCS.

* This work was supported by the US DOE under Contract No. W-7405-ENG-48.

+ Currently working on NIF site at Lawrence Livermore National Laboratories, Livermore, CA.

Sandia is a multi-program laboratory operated by Sandia Corporation, a Lockheed Martin Company, for the US DOE under Contract DE-AC04-94AL85000.

The effective circuit values for the PCS module, including the set of output cables, but not the flashlamps, are:

$$C = 6.24\ \text{mF} \quad R = 5.5\ \text{m}\Omega \quad L = 2.8\ \mu\text{H}$$

The following subsections describe the PCS components in more detail.

A. *High Energy Density Capacitors*

The metallized-dielectric, self-healing capacitors which are supplied by several sources are installed in two facing columns, or racks, each three capacitors wide and four high. The opening in the frame for each capacitor is 50.8 x 50.8 x 101.6 cm, sufficient to allow about 5-cm expansion in each dimension without hindering removal. The capacitors are insulated from the module frame by PVC trays, 0.32-cm thick, with a 5.7-cm lip. The nominal NIF bank is charged in approximately 60 s. Designing capacitors with an equivalent series resistance of <20 mΩ was an additional challenge for the vendors. The capacitor banks are electrically floating inside a 1-cm thick steel enclosure (E in Fig. 1), which is connected to facility ground. This protects personnel from direct exposure to the hazardous voltages. The enclosure and vented side panels serve the additional purpose of debris containment for the rare occasions when the large stored energy finds an alternative fault path to ground.

B. *Damping Elements*

Stainless steel coils with a mean diameter of 11.6 cm and a wire diameter of 1.43 cm serve to protect the capacitors from the rest of the bank for the case of an internal capacitor fault. These are covered by fiber cloth and epoxy reaching about 19.4 cm in diameter and 42.1 cm in length. The damping elements are sufficiently robust to maintain mechanical integrity after a major fault (up to 390 kA), although they would not be able to continue operating after that. They attach to the capacitor center conductor and the switch bus with 0.32-cm thick copper straps.

C. *High Voltage Bus and Dump Resistors*

The vertical bus is a 59.7-cm wide plate of 1.27-cm thick aluminum that tapers near the top to bolt to the lower switch plate. It is supported from the floor by two 1.27-cm G-10 plates. It is connected to the main bank power supply through a charge-isolation circuit. We added shelves to the bus to support the damping elements and dump resistors. The PCS module includes two independent safety dump assemblies; one is at the top and the other is at the bottom on the opposite side of the bus. Instead of the original single long stack (R in Fig. 1), each assembly is composed of two series stacks of eight, 15.2-cm diameter, 2.54-cm thick carbon composition discs from HVR Advanced Components. Each stack is 540 Ω with a decay time constant of about 3.4 s. A series connected Ross relay, with solenoids requiring ac voltage to open and spring drives for normal closing, is used to provide the fail-safe closure.

D. *Output Switch*

The output switch in Fig. 3 is a Maxwell PI ST-300A spark gap. It has a steel housing and 7-cm diameter poco-graphite electrodes with an initial gap of 0.32 cm. The switch dielectric medium is dry air, which flows through 5-micron filters. Extensive testing has resulted in a well-known self-break curve and very reliable operation at 40 to 50% of self-break. The air pressure is adjusted according to the predictable gap spacing as the electrodes erode due to the large 145-C charge transfer per shot. The switch end-of-life, as determined by reliable triggering range, occurs near 2,000 shots when the gap has grown to about 2.5 cm, for a total transfer of about 300 kC. The switch maintenance and refurbishment is simple.

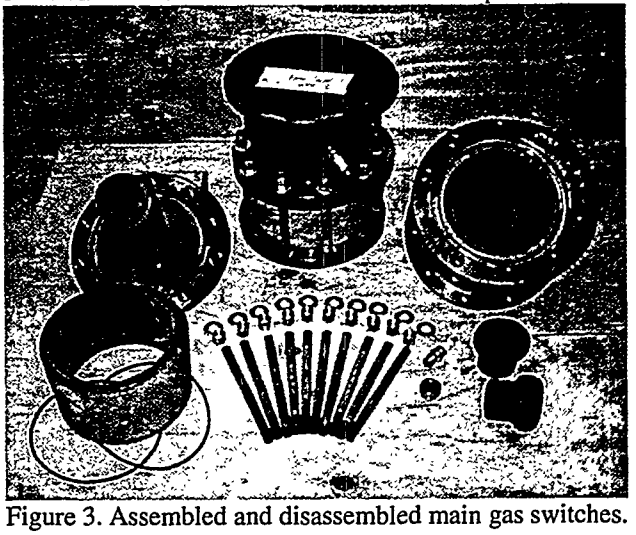

Figure 3. Assembled and disassembled main gas switches.

E. *Trigger Generator*

The trigger generator for the PCS output switch is a Maxwell PI TG-803-1, which was developed for this application. It uses an SCR for its main switch, pulse-charging an output capacitor through a pulse-transformer to approximately 95 kV. This capacitor is discharged through a sealed gas-filled spark-gap switch and an output blocking capacitor. The generator has a footprint of about 20.3 x 40.6 cm and is mounted on top of the module enclosure. Its high voltage bushing passes through a hole in the top plate. The trigger generator output has a Pulsed Power Components' high-current fuse connected in series before it enters the side of the module output switch via an automotive spark plug.

F. *Trigger Isolation Core*

The series-injection-trigger for the ST-300 switch requires at least 6 μH of inductance between the switch and the low-impedance load, to support the necessary trigger voltage. In FANTM this isolation is provided by a single Ceramic Magnetics' ferrite core, that is about 10.2-cm thick and has inner and outer diameters of 10.2 and 25.4 cm, respectively. The torus is split into two halves that are held together by plastic straps.

DISCLAIMER

G. Ballast Inductors

The set of 20 ballast inductors is attached to a common 1.27-cm thick aluminum plate, which is fed by the output switch through the isolation core. Copper coils with a mean diameter of 8.87 cm and a wire diameter of 0.65 cm are contained in a fiberglass-reinforced plastic. Fault currents of 100 to 190 kA represent worst-case conditions that the inductors are designed to survive mechanically. The assembly is enclosed by a 1.07-m diameter, top-hat shaped housing on top of the PCS module.

The ballast inductors serve the dual purposes of balancing the currents delivered to each output cable and load for a given module, plus matching the pulse shapes for all of the NIF modules with various cable lengths. Most modules will have only one associated cable length, and thus only one value for the set of ballast inductors. However, 24 modules will have two inductor values, due to the use of two different cable lengths to two different amplifiers that they are driving. The NIF module design calls for <30 μH of total inductance for the combination of the ballast inductor, cable, flashlamps, and all the output transitions and connections. Four different inductance values are recommended to compensate for the different inductance associated with each of the four ranges of cable lengths shown in Table 1.

Table 1. NIF Ballast Inductor Single-Pitch Design

Inductance(μH)	No. Turns	Cable Range(m)
19.1	25.5	19.8 – 27.7
17.5	23.5	27.7 – 38.1
14.3	19.5	38.1 – 48.2
12.8	17.5	48.2 – 54.9

H. Output Cables

Each module will drive a set of 20 RG-220 coaxial cables, one for each of 20 flashlamp pairs. The round-trip resistance of the cables represents a significant circuit parameter. Hence, for NIF a double-shield braid outer conductor configuration is suggested for cables shorter than about 38 m, and a triple-shield braid outer conductor configuration is suggested for cables longer than 38 m. This compensates somewhat for the higher resistance of the longest cables. On FANTM most of our testing has been with triple-braid cables that were 47.5 m long. Also, reinforcing the outer conductors with a fiber-backed mylar tape would ensure that the NIF cables will survive lamp faults of 100+ kA with no damage or degradation.

Since the modules with the longest cables probably cannot meet the NIF gain requirements when operating at the same charge voltage as the shorter systems, it was decided to allow for voltage adjustments on every module to achieve the best matching of performance. The gain improvement can be accomplished also through hand-selection of higher-capacitance cans for the higher loss modules, or just by adding a capacitor to the baseline bank of 20.

I. Resistor Dummy Loads

The dummy load assembly consisted of 20 independent floating resistor stacks. The 2-μH stacks were composed of five carbon composition discs from HVR Advanced Components that produced an average of 412 mΩ ±4% per stack, about 14% lower than the expected lamp operating resistance. They were air-cooled with large blower units to maintain a steady operating temperature. The loads performed well, but toward the end of their 7,200 shot series, the interface contacts were degrading, and several stacks had to be replaced.

J. NIF Flashlamp Loads

The FANTM facility includes 40 flashlamps uniquely designed for the NIF application by two vendors. They are housed in an air-cooled aluminum cabinet that roughly simulates the lamp cassette on NIF. The PCS output cables attach to connectors entering the top of the cabinet. The xenon-filled lamps are 1.8 m long with a diameter of 4.3 cm. Their nominal resistance at peak current and gain times is 476 mΩ ±8%. The amplitude and timing spreads due to lamp variations are mostly compensated by the PCS design.

K. PILC Module

The PILC bank and associated hardware are in a separate 0.61 by 1.52 by 1.98-m cabinet adjacent to the PCS module. It is connected through the PCS top-hat assembly with a series isolation resistor and an RG 220 coaxial cable, which should have a double or triple shield braid for fault tolerance. Typically, three parallel, inductively-isolated capacitors are discharged by a single air-insulated switch into the same load path seen by the PCS main bank. The nominal circuit values are 140 μF of capacitance driving a net series inductance of approximately 3.2 μH with a net series resistance of about 100 mΩ. Variations of this circuit can be charged from 24 to 28.5 kV to deliver between 500 and 700 J to each flashlamp. Like the main bank module, the PILC module is contained in an EMI enclosure with the pulsed power system electrically floating relative to the enclosure. The enclosure is tied to the facility ground, and the pulsed power ground is connected to the PCS pulsed power ground through the shield of the output coaxial cable.

L. Facility Grounding

The flashlamp load for the PCS module is isolated from facility ground, and the return current follows the cable outer conductors back to the main bank. The ground connection for the pulsed power system is at the PCS module where the module enclosure is tied to facility ground only at the top hat location with insulated leads. To minimize the risk of injury to NIF personnel, a low-inductance, effectively coaxial cable-tray return shall be used to surround the bundles of output cables between the modules and laser bays.

M. Diagnostics

The primary diagnostic tool is a current monitor located at the input of each of the twenty cables in the top-hat assembly. The SNL/EG&G developed monitor is a compact Rogowski coil which takes advantage of low cost printed circuit board technology. These current probes can be used to monitor the primary main and PILC current pulses as well as their triggers, plus ground and lamp reflector fault currents if they occur. The monitors were calibrated in situ using a single conductor to link them all with a certified reference current viewing resistor. A large Rogowski coil was used at the base of the ballast inductor assembly to measure the total current out of the main bank for a reference; this is not planned for the NIF modules.

The FANTM lamp voltage monitor (also not intended for NIF) is a 2000:10-Ω voltage divider with a 1:1 transformer to isolate the building and pulsed power grounds. Designed for this unique application, they were calibrated in situ on the 20 lamp loads against a certified reference monitor. Both the properly calibrated voltage and current monitors have demonstrated a shot-to-shot consistency of about ± 1%.

Our other primary diagnostic was video cameras that could observe the whole FANTM facility to document any off-normal occurrences. Alternatively, they could zoom onto specific spots of interest or meter displays as an aid in operations and troubleshooting.

N. Auto-Sequencing Controls

The main and PILC bank power supplies, main and PILC switch trigger generators, gas chassis and supply system, and diagnostic system were all monitored and controlled by an embedded control system. An auto-sequencing process was developed to allow repetitive firing of FANTM every five to six minutes. This allows for adequate switch purging and filling and avoids overheating any of the circuit elements. When the auto-sequencer detects all systems are ready, it initiates the next charging cycle and trigger pulse. The sequencing includes firing a lamp check PILC pulse only, between shots of the combined main bank plus PILC.

II. FANTM PERFORMANCE

The expected performance for the NIF main and power amplifiers drive the requirements for the PCS modules, which are listed in Table 2.

Table 2. PCS Module Pulsed Power Requirements

Module peak power to lamp set	≥ 300 MW
Power pulse width (10% points)	≤ 390 μs
Peak current (total)	≥ 490 kA
Peak current per lamp pair	≥ 24.5 kA
Energy per lamp pair	≥ 70 kJ
Shot-to-shot peak current variability	≤ ± 1%
Cable-to-cable peak current variability	≤ ± 3%
Pulse-to-pulse &unit-to-unit jitter	≤ 1 μs

A significant amount of circuit simulations (detailed Pspice models at Maxwell PI and SCREAMER[1] at SNL), field stress modeling (ELECTRO from Integrated Engineering Software), and gain code calculations (Bulkmode[2] and GainCalc V1.0[2] from LLNL) were conducted during the design and operation phase of the FANTM facility. SCREAMER is a fast-running, quick turn-around, user-friendly network code created and used extensively at Sandia for accelerator development. It requires some care in choosing a simplified representation of the system to be modeled. The codes from LLNL generated a time-dependent Average Gain Coefficient (AGC) from an input file consisting of the load power pulse, giving us an accurate estimate of the gain performance without having to drive a real amplifier. These tools provided us with redundant checks and guidelines for analyzing the performance data and to better understand any major or subtle deviations from the simulated predictions. Other software that was used extensively included the Lab View Data Viewer and Microsoft Excel.

The key performance parameter in the system is amplifier gain. The computer code developed by LLNL predicts the gain coefficient averaged over the set of flashlamps and the laser glass of the amplifier segment driven by a single PCS module, and includes such laser effects as Amplified Spontaneous Emission, which reduces gain when the power pulse is prolonged. The code has been benchmarked against the performance of several systems at LLNL, including the Beamlet Amplifier and AmpLab.[3]

A. Fixed Resistor Loads

The overlay of the PILC and main bank current waveforms in Fig. 4 shows the good agreement between the SCREAMER circuit model results and the measured data from FANTM shot # 4450. The primary difference is where the simulated curve does not damp out as fast for the PILC pulse. The measured waveform with a peak of 577 kA is actually the sum of all the individual cable Rogowski monitors when the main bank charge was 23.8 kV. The large total current Rogowski coil produces a slightly different wave shape because its physical location is such that it also measures the loss current into the discharged PILC circuit during the beginning of the main pulse.

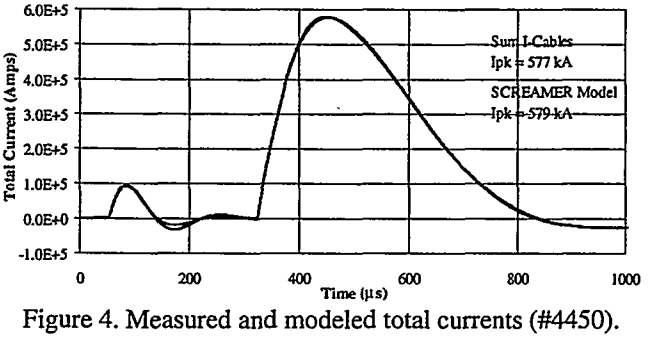

Figure 4. Measured and modeled total currents (#4450).

The shot-to-shot repeatability of the FANTM pulses satisfied the energy-spread requirements established for NIF. Figure 5 demonstrates the overall variation in peak main bank currents for a 500 shot series with the resistor loads. The horizontal bars represent the 1%-NIF energy spread requirement. Our power supplies showed a tendency to stabilize to a very repeatable charge voltage after about six shots. This temperature sensitivity causes a "first-shot" effect with lower peak values for the initial shot by about 0.5%. Even the larger scatter of the "first-shot" data still fell within the allowed energy window. The different plateaus on the plot correspond to changes in operating conditions, such as the set charge voltage.

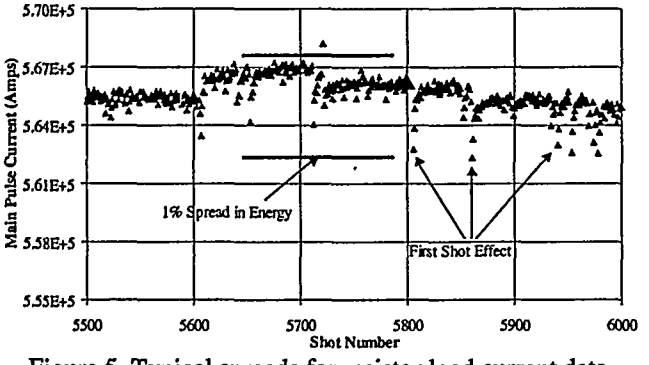

Figure 5. Typical spreads for resistor load current data.

B. *NIF Flashlamp Loads*

The FANTM fixed resistor loads and non-linear flashlamp loads produced significantly different waveforms when driven by the same source. Because of the time-varying impedance of the flashlamps and the geometry of the lamp holder, the shape of the power pulse delivered to the lamp pairs is shorter and broader than that of the resistor load. A comparison of the power waveforms from resistor shot #4450 and lamp shot #850 is shown in the overlay of Fig. 6. The lamp loads look more resistive and inductive.

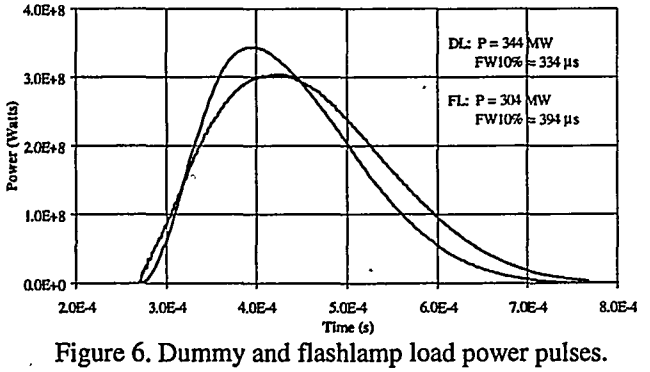

Figure 6. Dummy and flashlamp load power pulses.

Flashlamp Resistance

The flashlamp load impedance models that we use are approximate I-V relationships derived from breakdown physics, lamp geometry, and experience at LLNL[4]:

$$V_{L20} = 17.6\,(I_{L20})^{1/2} \qquad (1)$$

and

$$V_L = 78.7(I_L)^{1/2}. \qquad (2)$$

The Eq. 1 represents 20 series pairs of flashlamps, while Eq. 2 is for a single series pair. Measured flashlamp resistance departs significantly from this model late in time. This accurately predicts the minimum resistance value and the general profile, until the current begins to fall after the main pulse. The actual lamp resistance remains low for a considerable time, as the temperature and ionization of the gas in the lamp are still quite high. The measured flashlamp resistance shows a significant hysteresis that has not been included in the load resistance model. This hysteresis reduces the peak current and prolongs the time to peak current. However, it does not significantly alter the energy delivered to the lamps. From a circuit performance standpoint, it behaves very much like an additional series inductance of 12 µH per lamp set, more than the simple geometry would suggest. It was necessary to add this inductance-like correction to our circuit models to achieve good agreement between the simulations and actual data.

The graph of Fig. 7 compares a SCREAMER generated flashlamp load impedance, adjusted in time for the best fit, with a measured load resistance curve based on $R_L = V_L/I_L$ for a single lamp pair (#15) from lamp shot #850. The model matches the data best only near the time of peak current. Our resistance model both falls and recovers faster than the measured results indicate for the NIF lamps, which explains the differences between model and experiment. The Pspice simulations produced the same results.[5] The additional model inductance we required tends to serve as a construct to account for some of the dR/dt in the loads.

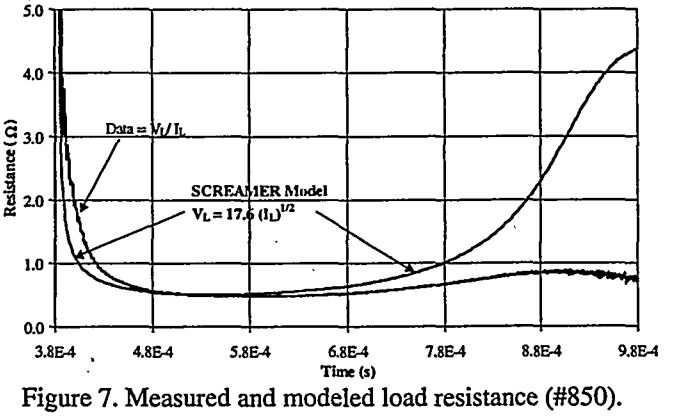

Figure 7. Measured and modeled load resistance (#850).

Figure 8 shows another total current comparison of a SCREAMER generated waveform (using the inductance-compensated circuit) and the sum of the cable currents for lamp shot #850, in which the bank was again charged to 23.8 kV. The simulated result is the lower curve for most of the plot. The fit is not quite as good as for the resistor dummy load, but it is sufficient to produce nearly identical gain calculations of 5.03 and 5.04 %/cm for the model and experiment, respectively.

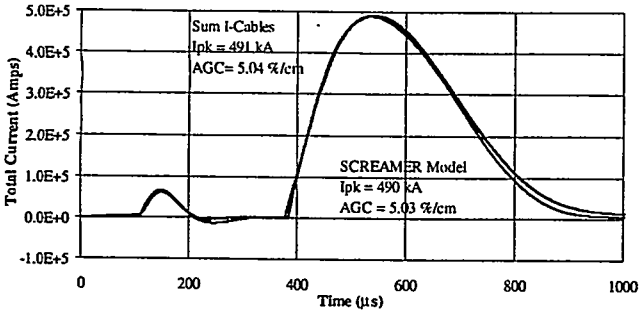

Figure 8. Measured and modeled total currents (L#850).

Reproducibility and Reliability

The lamp-to-lamp and shot-to-shot uniformity of the main pulse is indicated in Fig. 9. The peak currents seen by three flashlamp pairs are shown representing the highest, average, and lowest of the 20-load assembly over a 1150-shot series. The horizontal bars at the right of the graph show a 3% spread in energy. The data points indicated by the "No PILC" label are the result of firing the main bank only. The advantage of the PILC pre-ionization pulse in this case is about 600 A or 2.5%.

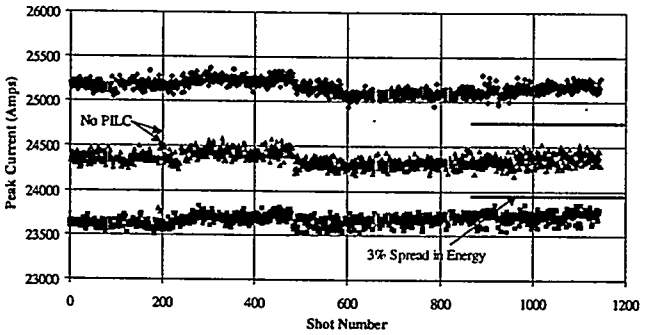

Figure 9. Peak current uniformity for three lamp pairs.

When all parameters were held constant, the result was very good reproducibility; the individual lamp shot-to-shot scatter is about 1%. The overall lamp-to-lamp spread appears to be about 6%, of which <2% would be accounted for by variations in the monitor calibrations.

A view of the lamp-to-lamp uniformity within a given shot on FANTM is shown in the bar chart of Fig. 10 for lamp shot #6153, which happens to be a "first shot" of the day. There is some shot-to-shot jitter of the calculated

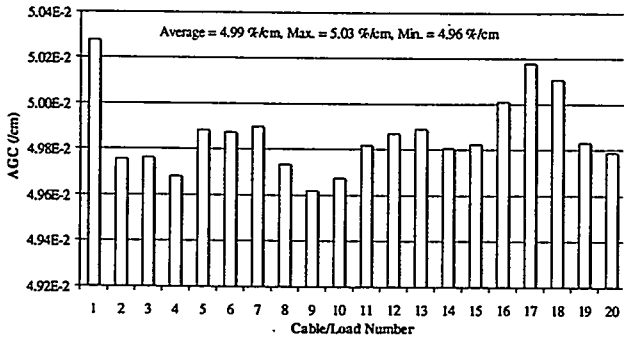

Figure 10. Lamp-to-lamp uniformity for lamp shot #6153.

AGC for each lamp pair, but the relative values of the different pairs are quite repeatable. Our investigations have shown that the lamp differences did not appear to depend on location or geometry in FANTM. The average AGC for all the loads on this shot is 4.99 %/cm, slightly below the desired parameter of 5.00 %/cm due to a gradual decline in the total bank current toward the end of the testing period.

As an example of load-to-load variability, the total spread of peak currents for FANTM shot #1320 was ±3.1%. The pulsed power system was determined to meet the cable-to-cable variability specification for identical loads, so the bulk of this spread is due to resistance differences between the lamp pairs. Measured data and predicted laser performance for shot #1320 are given in Table 3. A graphic example of the resistance profile variability for same three lamp loads is shown in Fig. 11.

Table 3. Results from FANTM Shot #1320

Cable/Lamp No.	9	15	17
AGC (%/cm)	5.046	5.032	5.002
Lamp Pair Energy (kJ)	73.3	72.8	71.2
Peak Current (kA)	25.2	24.7	23.8
R_{min} (Ω)	0.453	0.478	0.509
$R_{min} \times I_{pk}^{1/2}$	71.9	75.1	78.5

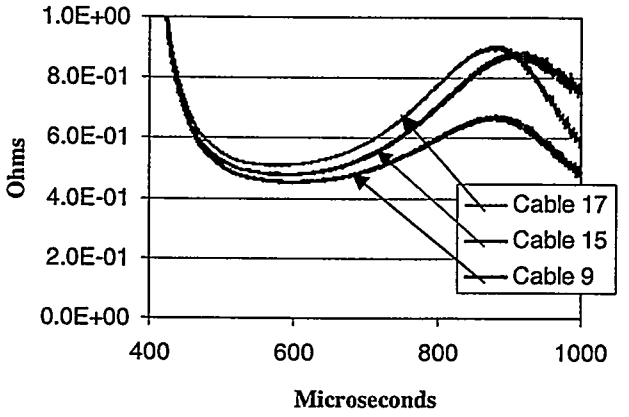

Figure 11. Three FANTM load resistance profiles.

Parameter Sensitivity

In the parameter range of interest, system gain is nearly linearly proportional to energy delivered to the flashlamps, and is weakly dependent on peak power, with gain being slowly reduced as pulses get longer. Flashlamp energy is, of course, dependent on the energy stored in the PCS module and that lost in series resistance. Ultimately the energy delivered to the load depends on charge voltage and bank capacitance, or the number of capacitors. We ran a series of tests on FANTM in which we varied both parameters. Calculating the gain for selected shots and displaying it as in Fig. 12 allows us to identify gain contours and estimated scale factors as an aid for tuning future PCS module/cable/amplifier

combinations. The resulting voltage impact on gain goes as 62 V / 0.01 %/cm. The scaling for capacitance looks like 1 Cap(310 μF) / 0.06 %/cm. Both relationships appear close to linear in this small range of variables. The gain contours associated with modules that drive shorter cables should shift left and down with respect to those of Fig. 12 because of the associated lower losses.

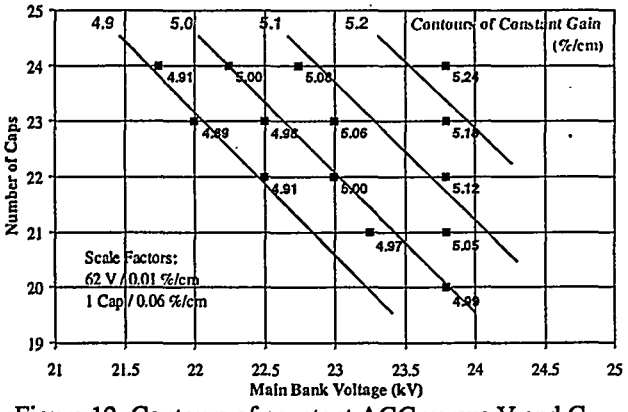

Figure 12. Contours of constant AGC versus V and C.

The AGC also demonstrates some sensitivity to the to the PILC energy, the pre-ionization pulse shape, and the delay time between the PILC pulse and the main bank pulse. These effects have been evaluated over the limited range of parameters available with the FANTM facility.[5] The optimum delay appears to be between 250 and 400 μs. Higher PILC energies tend to maintain the optimum near the peak for a greater range of delay times. The minimum acceptable energy delivered to each lamp is about 550 J. The preferred operating point for the PILC bank would appear to be about 28.5 kV or about 650 J/lamp. This would provide some margin for the variations in pre-ionization energies and lamps.

Since the measured power pulse on FANTM matches well with the modeled results (after the added inductance to model the hysteresis), it should be no surprise that the AGC inferred from FANTM tests matches well with the predicted results, as shown in Table 4.

Table 4. Modeled and Measured Performance

	PSpice	FANTM
Module peak power	299 MW	300 MW
Power pulse (10% points)	392 μs	390 μs
Peak current per lamp pair	24.4 kA	24.6 kA
Energy per Lamp Pair	74.6	73 kJ
Average Gain Coefficient	5.05 %/cm	5.02 %/cm

III. PREDICTED AND MEASURED FAULT CONDITIONS

A complete summary of our fault analysis and plans is beyond the intent of this section, but some discussion is deemed appropriate. During the course of the FANTM testing, we experienced three major capacitor faults (ranging from 11 to 23.8 kV), one bus fault through a damaged dump resistor, and one lamp fault. Due to the large number of energized components that will be in NIF, some failures have to be expected, but with the risks minimized and contained. We conducted intentional faults at the end of our test series on a prototype bank to diagnose the fault current and voltage levels. Of particular interest are the possible threats to personnel safety or collateral property damage. Every component on FANTM was considered with respect to the likely and unlikely fault modes that it would be exposed to, or could cause. As an example, the damping elements were designed by considering the trade-off between the loss they cause for normal operation and the maximum fault current they would pass. Figure 13 shows a plot of the normal current and fault current both as a function of the damping element inductance

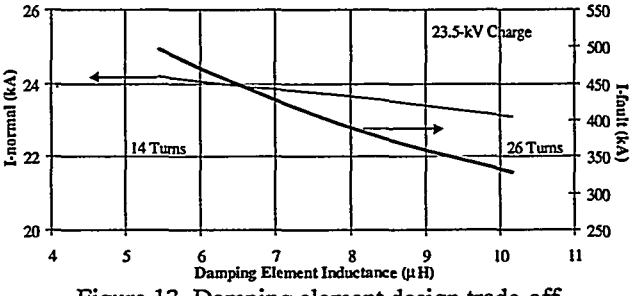

Figure 13. Damping element design trade-off.

An overlay of some of the fault currents our models predict is shown in Fig. 14. The plotted curves represent a bus breakdown to ground, a capacitor internal short, a cable or feed-connector failure at the top-hat assembly, and a lamp failure or Big-Tee connector short near the load. All the curves except the bus fault are associated

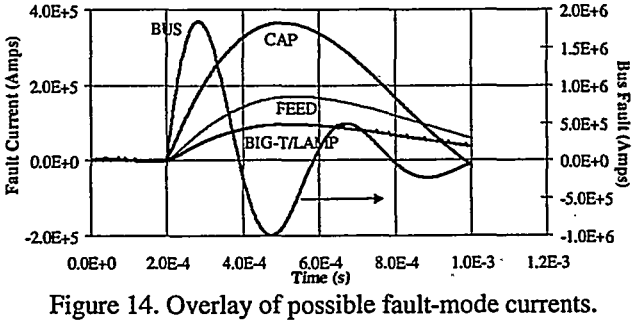

Figure 14. Overlay of possible fault-mode currents.

with the left-side scale, while the bus fault requires the right-side scale. Obviously, the possibility of a bus fault is a failure mode that we want to make statistically remote, because it produces the highest current released and potential for the most damage. The curves of Fig. 14 are generated for specific circuit conditions and assuming a fault-path resistance of 5 to 10 mΩ. Our experiences with planned faults on the prototype bank have indicated higher resistances. The resulting actual peak values could vary significantly (e.g. –50% to +10%). For instance, our one lamp failure drew a fault current that peaked to about 45 kA, about half of the peak value indicated in Fig. 14.

IV. SUMMARY

We have designed, modeled, fabricated, and tested the First Article NIF Test Module. Measurements made during tests of the FANTM module have confirmed the basic predictions of the NIF performance models, and have allowed a further refinement of the models, particularly in the area of the hysteresis of the flashlamp resistance profile. We conducted evaluations under a variety of normal and fault conditions in order to make final design refinements. With our experience in developing this Power Conditioning System over its near lifetime-equivalent series of tests, we think it should meet NIF requirements for performance, cost, and compactness, with the flexibility to exceed some of the specifications.

V. ACKNOWLEDGEMENTS

The authors wish to express their appreciation to all the contributors on the PCS team. These include Doug Larson, Mark Newton, Steve Fulkerson, Scot Hulsey, and Dave Pendleton at LLNL; Ed Weinbrecht, John Boyes, Dennis Muirhead, Dave VanDeValde, and Ellis Dawson at SNL; Bob Anderson of American Control Engineering; Bill Gagnon of LLNL. Our thanks are also due to the members of the FANTM operations crew, Gary Mowrer, Jacob Adcock, Bob Nichols, and Ray Gignac. All were responsible for the culmination of this project and paper.

VI. REFERENCES

[1] M. L. Kiefer and M. M. Widner, "SCREAMER – A Pulsed Power Design Tool, User's Guide," in *Digest of Tech. Papers, 5th IEEE Pulsed Power Conf.*, eds. M. F. Rose and P. J. Turchi, 1985, p. 685.

[2] Private communications with Ken Jancaitis, LLNL.

[3] H. T. Powell, A. C. Erlandson, K. S. Jancaitis and J. E. Murray, "Flashlamp Pumping of ND:Glass Disk Amplifiers," SPIE 1277, p103 (1990)

[4] J. H. Goncz, *J. Appl. Phys.*, vol. 36, p. 742, 1994.

[5] J. Hammon, E. S. Fulkerson, D. L. Smith, J. M. Wilson, H. C. Harjes, and W. B. S. Moore, Paper PB034, *Proc. 12th IEEE Pulsed Power Conf.*, 199